Journal of Nutrition and Health Sciences
Volume 6 | Issue 1
ISSN: 2393-9060

Research Article Open Access

Solid State Characterization of the Consciousness Energy Healing Treated Ferrous Sulphate

Trivedi D[1] and Jana S[*2]

[1]Trivedi Global, Inc., Henderson, USA
[2]Trivedi Science Research Laboratory Pvt. Ltd., Thane, India

[*]**Corresponding author:** Jana S, Trivedi Science Research Laboratory Pvt. Ltd., Thane (W), India, Tel: +91-022-25811234, E-mail: publication@trivedieffect.com

Citation: Trivedi D, Jana S (2019) Solid State Characterization of the Consciousness Energy Healing Treated Ferrous Sulphate. J Nutr Health Sci 6(1): 102

Received Date: March 27, 2019 **Accepted Date**: April 26, 2019 **Published Date:** April 29, 2019

Abstract

Ferrous sulphate is an inorganic iron salt used for the prevention and treatment of iron deficiency anaemia. The study aimed to evaluate the effects of the Trivedi Effect®- Consciousness Energy Healing Treatment on the solid state properties of ferrous sulphate using sophisticated analytical techniques. The test compound, ferrous sulphate was divided into two parts and named as the control and treated sample. The control ferrous sulphate did not receive Biofield Energy Treatment; however, the Treated sample received the Trivedi Effect®-Consciousness Energy Healing Treatment remotely by the well-known Biofield Energy Healer, Dahryn Trivedi (USA) for 3 minutes. The PXRD relative peak intensities and crystallite size of the treated sample were significantly changed from -66.93% to 331.88% and -24.92% to 139.87%, respectively compared with the control sample. The particle size in the treated sample values were significantly decreased by 17.56% (d_{10}), 26.94% (d_{50}), 31.66% (d_{90}), and 28.98% {D(4,3)}, respectively; however, the specific surface area was significantly increased by 29.57% compared to the control sample. The melting point of the treated ferrous sulphate in the 1st and 3rd peaks was decreased by 4.06% and 2.55% respectively, while increased by 8.40% and 0.17% in the 2nd and 4th peaks, respectively compared to the control sample. The total latent heat of fusion was significantly decreased by 23.22% in the treated sample compared with the control sample. The total weight loss in the treated ferrous sulphate was increased by 2.00% compared with the control sample. The maximum thermal decomposition temperature of the treated ferrous sulphate was decreased by 2.14%, 16.53%, 3.89%, and 2.21% in the 1st, 2nd, 3rd, and 4th peak respectively, compared to the control sample. The Biofield Energy Treatment might lead to the production of a new polymorphic form of iron sulphate. The Biofield Energy Treated ferrous sulphate would be useful to design more efficacious nutraceutical/pharmaceutical formulations, which might offer better therapeutic response against iron deficiency anaemia.

Keywords: Iron Sulphate; Consciousness Energy Healing Treatment; Trivedi Effect®; PXRD; PSA; DSC; TGA/DTG

Introduction

Ferrous sulphate or iron (II) sulphate is an inorganic salt of iron, an industrial mineral [1]. It usually remained in various states of hydration with the formula $FeSO_4 \cdot xH_2O$. This salt is also known as "green vitriol" and "copperas" since from the ancient time. These salts exist mostly in heptahydrate ($FeSO_4 \cdot 7H_2O$) form or also known as melanterite [2,3]. Ferrous sulphate is very useful as a medicine for the treatment of iron deficiency anaemia [4]. Besides, it is also used as a dye and in preparation of inks. In horticulture ferrous sulphate is usually used for the treatment of iron chlorosis and wood panelling; in gold refining, water purification and also for identification of mushrooms; as lawn conditioner, moss killer, photographic developer, and a catalyst (Fenton's reagent) in various chemical reactions [3,5-7]. Problems associated with the internal use of ferrous sulphate are stomach upset, constipation, black/dark-coloured stools, and staining of the teeth. It is in water (29.51 g/100 mL at 25 °C) and negligible in organic solvents [3,8]. The complex physiological system of the human body and other dietary factors, only 1-2 mg of iron undergoes absorption through the gut enterocyte to the systemic circulation [9,10]. Iron deficiency is the most common nutritional disorder affecting more than 20% of the global population according to the World Health Organization (WHO). Dietary iron bioavailability is low in our body due to the impaired iron absorption from the dietary iron supplement and iron fortified food [11]. The Trivedi Effect®- Consciousness Energy Healing Treatment has been found to be effective for the reduction of particle size and crystallite size with the improvement of the surface area that would be helpful for the enhancement of the solubility and bioavailability of pharmaceutical/nutraceutical compounds [12-14].

Biofield Energy (also defined as quantum energy matrix) is an electromagnetic field present in the surround of the human body resulting from the continuous movement of the electrically charged components (ions, cells, etc.). Biofield Energy is believed to

correlate with the living force, which is the source of life and has been known as prana by the Hindus, qi or chi by the Chinese and ki by the Japanese from the ancient time. The Biofield Energy Healers have the capability to harness the energy from the "Universal Energy Field" and can transfer into any living or non-living object(s). The process by which the objects receive the Biofield Energy Treatment from the Biofield Energy Healer(s) and respond into a useful way is called as Biofield Energy Healing Treatment. The Biofield Energy Healing therapy has been acknowledged as a Complementary and Alternative Medicine (CAM) health care approach for the improvement the quality of life by the National Center of Complementary and Integrative Health with other therapies, medicines and practices such as Qi Gong, yoga, chiropractic/osteopathic manipulation, cranial sacral therapy, Tai Chi, meditation, healing touch, homeopathy, acupuncture, acupressure, hypnotherapy, naturopathy, movement therapy, Ayurvedic medicine, aromatherapy, Reiki, etc. [15,16]. Biofield Energy Healing Treatment is drawing importance in different scientific fields include material science, pharmaceuticals, nutraceuticals, organic compounds, microbiology, agricultural, biotechnology, genetics medical [17-33]. The solid state properties like physicochemical and thermal properties of a pharmaceutical compound play an important role in drug performance, i.e. bioavailability, therapeutic efficacy, and toxicity [34,35]. The Trivedi Effect® claimed to be modifying the physicochemical and thermal properties through the possible intervention of neutrinos [36]. Thus, it was designed to investigate the effects of the Trivedi Effect® - Consciousness Energy Healing Treatment on the solid properties such as physicochemical and thermal properties of ferrous sulphate using modern analytical techniques.

Materials and Methods

Chemicals and Reagents

Ferrous sulphate Heptahydrate {iron (II) sulphate Heptahydrate} (>99%) was purchased from Sigma-Aldrich and other chemicals used during the experiments also purchased in India.

Consciousness Energy Healing Treatment Strategies

The test compound, ferrous sulphate was divided into two parts and named as the control and Biofield Energy Treated sample. The control ferrous sulphate did not receive Biofield Energy Treatment. But, the sample was subjected to a "sham" healer, who did not have any knowledge about the Biofield Energy Treatment. The Biofield Energy Treated sample received the Trivedi Effect® -Consciousness Energy Healing Treatment remotely by the well-known Biofield Energy Healer, Dahryn Trivedi (USA) for 3 minutes. After that, both the sample was kept in similar sealed conditions and characterized using sophisticated analytical techniques.

Characterization

The powder X-ray diffraction (PXRD) analysis of ferrous sulphate powder sample was performed with the help of PANalytical X'PERT3 powder X-ray diffractometer (UK) [12-14]. The average size of crystallites ferrous sulphate powder was calculated from PXRD data using the Scherrer's formula (1)

$$G = k\lambda/\beta\cos\theta \quad (1)$$

Where k is the equipment constant, λ is the radiation wavelength, G is the crystallite size in nm, β is the full-width at half maximum, and θ is the Bragg angle [37].

The particle size analysis (PSA) was performed using Malvern Mastersizer 3000 (UK) using the wet method [12-14]. Similarly, the differential scanning calorimetry (DSC) analysis of ferrous sulphate was performed with the help of DSC Q2000 differential scanning calorimeter (USA). The thermogravimetric analysis (TGA) thermograms of ferrous sulphate were obtained with the help of TGA Q500 themoanalyzer (USA) apparatus [12-14].

The % change in the peak intensity, crystallite size, particle size, specific surface area, latent heat, melting point, weight loss and the maximum thermal degradation temperature of the treated sample was calculated compared with the control sample using the following equation 2:

$$\% \text{ Change} = \frac{[\text{Treated-Control}]}{\text{Control}} \times 100 \quad (2)$$

Results and Discussion

Powder X-ray Diffraction (PXRD) Analysis

PXRD diffractograms of both the ferrous sulphate sample displayed sharp and intense peaks (Figure 1) indicating that the samples were crystalline. The crystallite size was calculated with the help of Scherrer equation [37]. The PXRD data of both the samples are presented in Table 1. The highest intense peak in the control sample was observed at Bragg's angle (2θ) equal to 23.7° (Table 1, entry 6). While the highest intense peak was found in the Biofield Energy Treated sample at 2θ equal to 18.2° (Table 1, entry 3). The Bragg's angle (2θ) of the 11 diffraction peaks in both the samples remained almost same, but the relative intensities of the

peaks of the Biofield Energy Treated sample were found to be altered compared to the control sample. The relative intensities at 2θ equal to 16.3°, 16.8°, 18.2°, 19.6°, 22.2°, 23.9°, and 32.9° (Table 1, entry 1-5, 7, and 11) in the Biofield Energy Treated sample were significantly increased from 5.40% to 331.88% compared to the control sample. Subsequently, the relative intensities of the PXRD peaks at 2θ equal to 23.7°, 27.5°, 27.9°, and 32.6° in the Biofield Energy Treated sample were significantly decreased from 14.17% to 66.93% compared to the control sample (Table 1, entry 6 and 8-10). The crystallite size values of the treated sample at 2θ equal to 16.3°, 18.2°, and 27.9° was significantly reduced from 12.50% to 24.92% with respect to the control sample (Table 1, entry 1, 3, and 9). Consequently, the crystallite size values of the control and Biofield Energy Treated ferrous sulphate at position 2θ equal to 16.8°, 23.7°, and 27.5° remained unchanged (Table 1, entry 2, 6, and 8). Subsequently, the crystallite size values of the Biofield Energy Treated samples at 2θ equal to 19.6°, 22.2°, 23.9°, 32.6°, and 32.9° (Table 1, entry 4, 5, 7, 10, and 11) were significantly

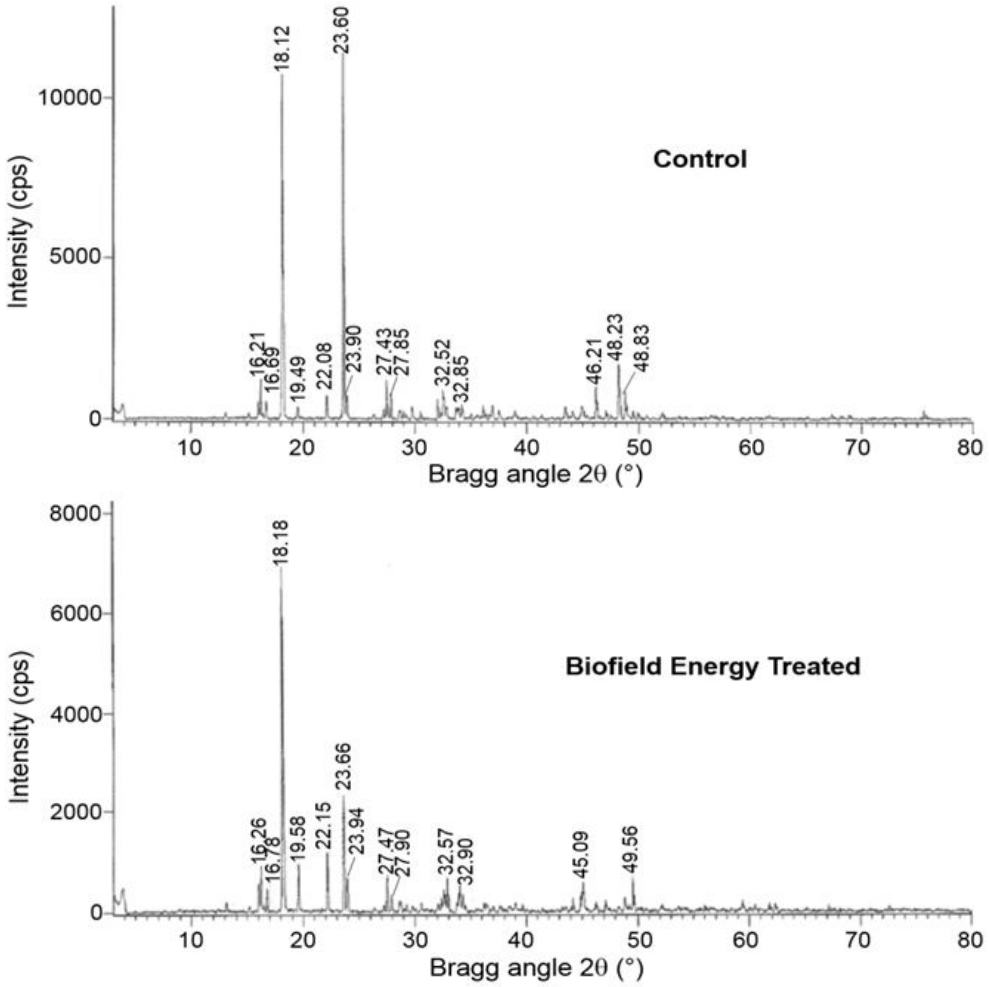

Figure 1: PXRD Diffractograms of the Control and Treated Iron Sulphate

Entry No.	Bragg angle (°2θ)	Relative Intensity (%)			Crystallite size (G, nm)		
		Control	Treated	% change	Control	Treated	% change
1	16.3	10.56	16.38	55.11	57.89	43.46	-24.92
2	16.8	5.11	6.81	33.27	49.71	49.71	0.00
3	18.2	94.88	100.00	5.40	58.04	49.81	-14.18
4	19.6	3.20	13.82	331.88	38.80	49.91	28.62
5	22.2	6.26	17.02	171.88	38.96	43.84	12.53
6	23.7	100.00	33.07	-66.93	50.24	50.25	0.01
7	23.9	6.80	9.67	42.21	43.98	50.28	14.31
8	27.5	11.29	9.69	-14.17	50.63	50.63	0.00
9	27.9	7.12	4.83	-32.16	50.67	44.34	-12.50
10	32.6	8.20	6.58	-19.76	71.65	89.58	25.02
11	32.9	3.50	9.85	181.43	29.90	71.72	139.87

Table 1: PXRD Data for the Control and Treated Iron Sulphate

increased from 12.53% to 139.87% in the treated sample in comparison to the control sample. The overall crystallite size of the Biofield Energy Treated ferrous sulphate was significantly changed from -24.92% to 139.87% compared with the control sample. The sharp and intense peaks at 2θ = 46.21°, 48.23°, and 48.83° in the control sample were found to be moved and reduced at 2θ = 45.09° and 49.56° in the Biofield Energy Treated Sample.

It has been recently reported that Biofield Energy Treatment has the significant ability to produce a new crystalline polymorph by changing the crystal morphology of the pharmaceuticals and nutraceuticals through altering the relative intensities and crystallite size of the diffraction peaks [38]. The variations in the crystallite size and relative intensities indicated the modification of the crystal morphology of the Biofield Energy Treated ferrous sulphate compared with the control sample. The Trivedi Effect®- Consciousness Energy Healing Treatment perhaps produced a new polymorph through the energy transferred into ferrous sulphate. Polymorphic forms of pharmaceuticals have the significant effects on the drug performance, because their thermodynamic and physicochemical properties like melting point, energy, stability, and especially solubility, are different (probably improvement) from the original form [39,40]. Thus, it can be anticipated that Dahryn's Biofield Energy Treatment could be a very useful method for the production of novel crystal polymorph that would offer an improved on its therapeutic performance.

Particle Size Analysis (PSA)

The particle size and specific surface area of the control and treated ferrous sulphate were investigated and presented in Table 2. It was observed that the particle size in the Biofield Energy Treated sample at d_{10}, d_{50}, d_{90} and D (4,3) values were significantly decreased by 17.56%, 26.94%, 31.66%, and 28.98%, respectively compared to the control sample (Table 2). The specific surface area of the treated ferrous sulphate was meaningfully increased by 29.57% compared with the control sample. It is presumed that the Trivedi Effect® might act as an exterior force for tumbling the particle size of ferrous sulphate. Scientific literature mentioned that a pharmaceutical solid compound having reduced particle size with an improvement surface area possesses enhanced solubility, absorption, dissolution rate, and finally bioavailability [41,42]. Thus, it is anticipated that the treated sample might offer better bioavailability than the untreated sample.

Test Item	d_{10} (µm)	d_{50} (µm)	d_{90} (µm)	D(4,3) (µm)	SSA(m^2/Kg)
Control sample	131	386	998	490	22.86
Biofield Energy Treated	108	282	682	348	29.62
Percent change (%)	-17.56	-26.94	-31.66	-28.98	29.57

d_{10}, d_{50}, and d_{90}: particle diameter of the cumulative distribution, D (4,3): the average mass-volume diameter, and SSA : the specific surface area.
Table 2: Particle Size Distribution of the Control and Treated Iron Sulphate

Differential Scanning Calorimetry (DSC) Analysis

Scientific literature reported the dehydration behavior of a hydrated iron salt, ferrous sulphate heptahydrate ($FeSO_4•7H_2O$) by using DSC and TGA techniques [43,44]. Wang *et al.* mentioned 3 peaks in the DSC curve at a heating rate of 10 °C under nitrogen atmosphere. 1st peak at temperature below 100 °C, 2nd peak at 85 to 149 °C, and 3rd peak at 247 to 342 °C were due to the dehydration of 7 water molecules from $FeSO_4•7H_2O$ to $FeSO_4•4H_2O$, $FeSO_4•4H_2O$ to $FeSO_4•H_2O$, and $FeSO_4•H_2O$ to $FeSO_4$, respectively. They also concluded that accurate thermal data from the TGA/DSC dehydration experiments depends on various factors like proper selection of the heating rate, particle size, open or closed pan, etc. [43].

The DSC thermogram of the control ferrous sulphate heptahydrate showed the presence of the four endothermic peaks at 71.46, 88.95, 118.44, 271.63 °C (Figure 2). The 1st sharp endothermic peak at 71.46 °C was the melting point of ferrous sulphate heptahydrate. Consequently, the melting temperature of Biofield Energy Treated sample was significantly decreased by 4.06% with a significant enhancement of the latent heat of fusion (ΔH) by 52.67% compared with the control sample (Table 3). The 2nd broad endothermic peak at 88.95 °C might be due to the dehydration of 2 molecules of water from $FeSO_4•6H_2O$ to $FeSO_4•4H_2O$. This endotherm temperature in the Biofield energy Treated sample (88.95 °C) was significantly increased by 8.40% with a significant enhancement in ΔH by 291.62% compared with the control sample. The melting temperature of the 3rd sharp endothermic peak, which was due to the removal of 3 molecules of water from $FeSO_4•4H_2O$ to $FeSO_4•H_2O$ was decreased in the Biofield Energy Treated sample (115.42 °C) by 2.55% with a significant reduction in ΔH by 69.46% compared with the control sample (118.44 °C). Finally, a broad endothermic peak at 271.63 °C was found in the control sample due to the dehydration from ferrous sulphate monohydrate to anhydrous $FeSO_4$. This melting temperature was increased by 0.17% in the Biofield Energy Treated sample (272.10 °C) with a significant enhancement in ΔH by 4.39% compared with the control sample (Table 3). The total latent heat of fusion to transition from $FeSO_4•7H_2O$ to $FeSO_4$ was significantly decreased by 23.22% in the Biofield Energy Treated sample (906.72 J/g) compared with the control sample (696.20 J/g). The reduction in the latent heat of fusion can be attributed to the disrupted molecule chains and reduced the crystallization structure [41,45]. Thus, it is assumed that Dahyrn's Biofield Energy treatment may be responsible for the disruption the molecular chains and crystallization structure of ferrous sulphate. The DSC analysis suggested that the thermal stability of the Biofield Energy Treated ferrous sulphate heptahydrate was decreased compared with the control sample.

Sample	Melting Temperature (°C)				ΔH (J/g)			
	1st Peak	2nd Peak	3rd Peak	4th Peak	1st Peak	2nd Peak	3rd Peak	4th Peak
Control Sample	71.46	88.95	118.44	271.63	64.19	40.83	539.70	262.00
Biofield Energy Treated	68.56	96.42	115.42	272.10	98.00	159.90	164.80	273.50
% Change*	-4.06	8.40	-2.55	0.17	52.67	291.62	-69.46	4.39

ΔH: Latent heat of fusion, *denotes the percentage change of the treated sample with respect to the control sample.
Table 3: The melting point (°C) and latent heat of fusion (J/g) values for both control and treated samples of iron sulphate

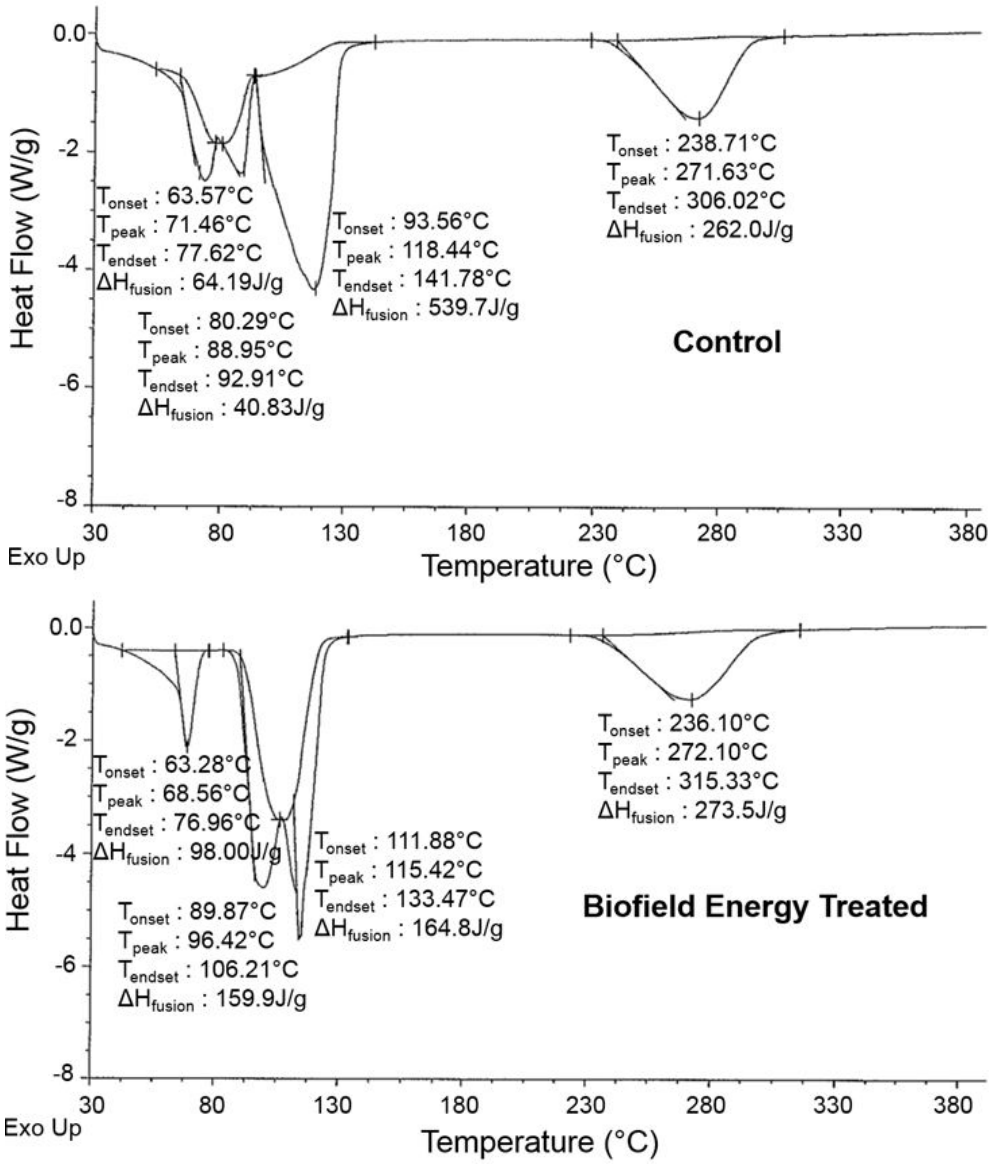

Figure 2: DSC Thermograms of the Control and Treated Ferrous Sulphate

Thermal Gravimetric Analysis (TGA) / Differential Thermogravimetric Analysis (DTG)

The TGA thermogram pattern of the control sample was matching with the literature. The first weight loss occurs between 70 and 90 °C due to the loss of 3 water molecules from $FeSO_4 \bullet 7H_2O$. The second dehydration step with the loss of 3 water molecules from $FeSO_4 \bullet 4H_2O$ is responsible for the mass loss between 140 and 200 °C. Consequently, the third weight loss is found between 270 and 350 °C due to the dehydration of $FeSO_4 \bullet H_2O$. Final major weight loss between 400 and 830 °C occurs due to the oxidation and dehydration of the other part of monohydrate, sulphate decomposition. The major weight loss occurred in the first (38.30%) and fourth (28.30%) reactions [43,44].

Here, the TGA thermograms of the control and Biofield Energy Treated samples exhibited four steps of thermal degradation, which was matched with the literature (Figure 3) [43,44]. The % weight loss in the Biofield Energy Treated ferrous sulphate was significantly increased by 69.50% in the 1st step of degradation compared with the control sample. On the other hand, the % weight

loss in the 2nd, 3rd, and 4th steps of degradation was significantly reduced by 2.58%, 21.09%, and 5.63%, respectively, compared with the control sample (Table 4). The total % weight loss of the control and Biofield Energy Treated ferrous sulphate were 71.06% and 71.5%, respectively. The total weight loss in the Biofield Energy Treated ferrous sulphate was increased by 2.00% compared to the control sample.

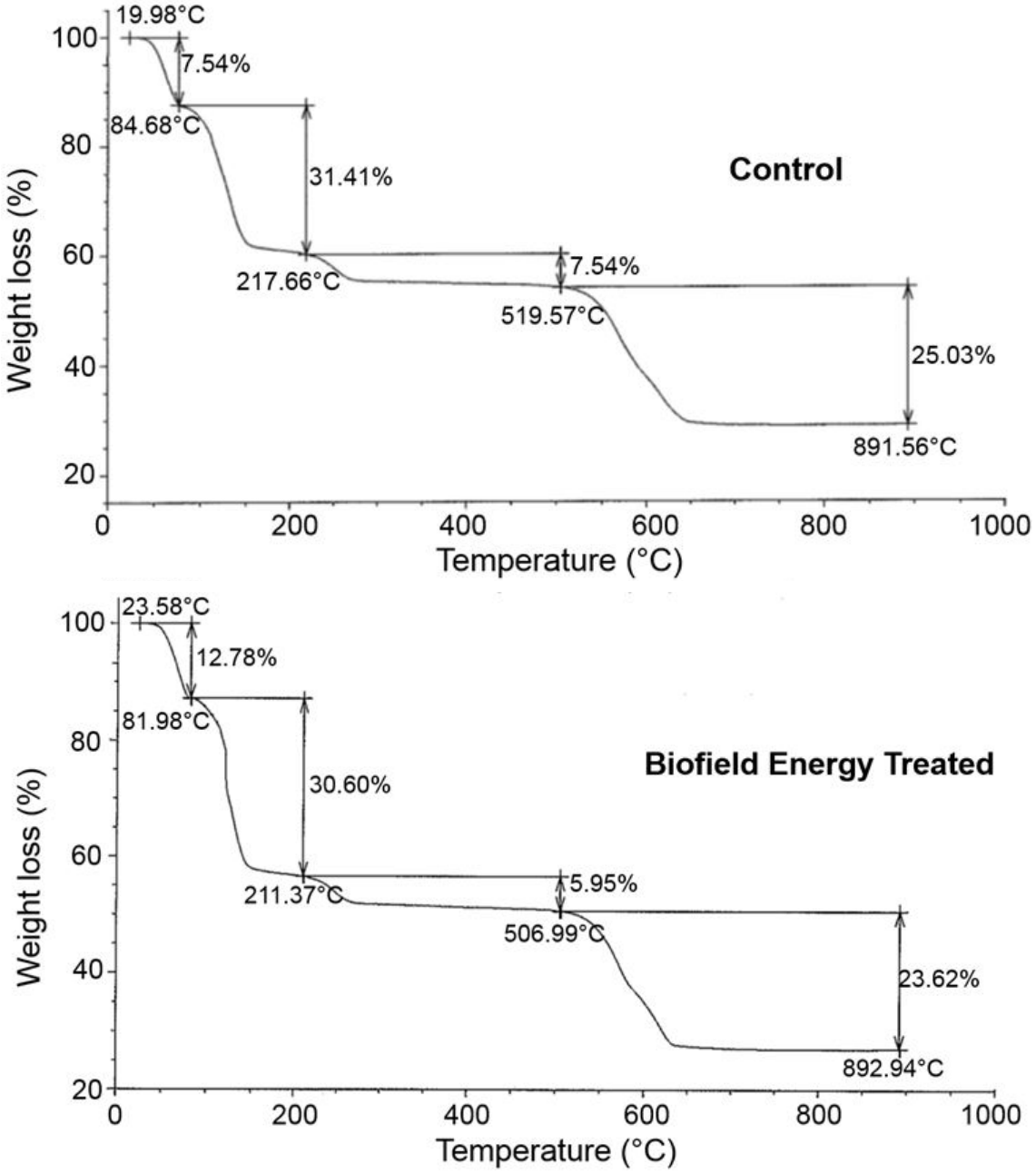

Figure 3: TGA Thermograms of the Control and Treated Iron Sulphate

Description	%Weight Loss				
	1st step	2nd step	3rd step	4th step	Total
Control Sample	7.54	31.41	7.54	25.03	71.52
Biofield Energy Treated sample	12.78	30.6	5.95	23.62	72.95
% Change	69.50	-2.58	-21.09	-5.63	2.00

Table 4: Thermal Degradation Steps of the Control and Treated Samples of Ferrous Sulphate

The DTG thermograms of the control sample disclosed four peaks P_1, P_2, P_3, and P_4 with maximum thermal decomposition temperature (T_{max}) of 68.76, 144.36, 256.03, and 585.59 °C, respectively (Figure 4 and Table 5). Similarly, the DTG thermograms of the Biofield Energy Treated sample disclosed four peaks P_1, P_2, P_3, and P_4 with T_{max} of 67.29,120.50, 246.08, and 572.65 °C, respectively (Figure 4 and Table 5). The analysis indicated that the T_{max} of the Biofield Energy Treated ferrous sulphate was

decreased by 2.14%, 16.53%, 3.89%, and 2.21% in the 1st, 2nd, 3rd, and 4th peak respectively, compared to the control sample. As per the literature, with alteration of the particle size changed the thermal stability of a sample [45]. Overall, TGA/DTG revealed that the thermal stability of the Biofield Energy Treated ferrous sulphate was reduced as compared to the control ferrous sulphate. The reduced thermal stability favours the enhanced dissolution rate and bioavailability of the pharmaceutical solid compound [40]. The result was well supported by the results of particle size analysis.

Description	T_{max} (°C)			
	P_1 (°C)	P_2 (°C)	P_3 (°C)	P_4 (°C)
Control Sample	68.76	144.36	256.03	585.59
Biofield Energy Treated	67.29	120.50	246.08	572.65
% Change	-2.14	-16.53	-3.89	-2.21

P_1, P_2, P_3, and P_4: peak 1, 2, 3, and 4. T_{max} = the temperature at which maximum weight loss takes place in TG or peak temperature in DTA.

Table 5: The Maximum Thermal Degradation Temperatures (T_{max}) of the Control and Treated Samples of Iron Sulphate

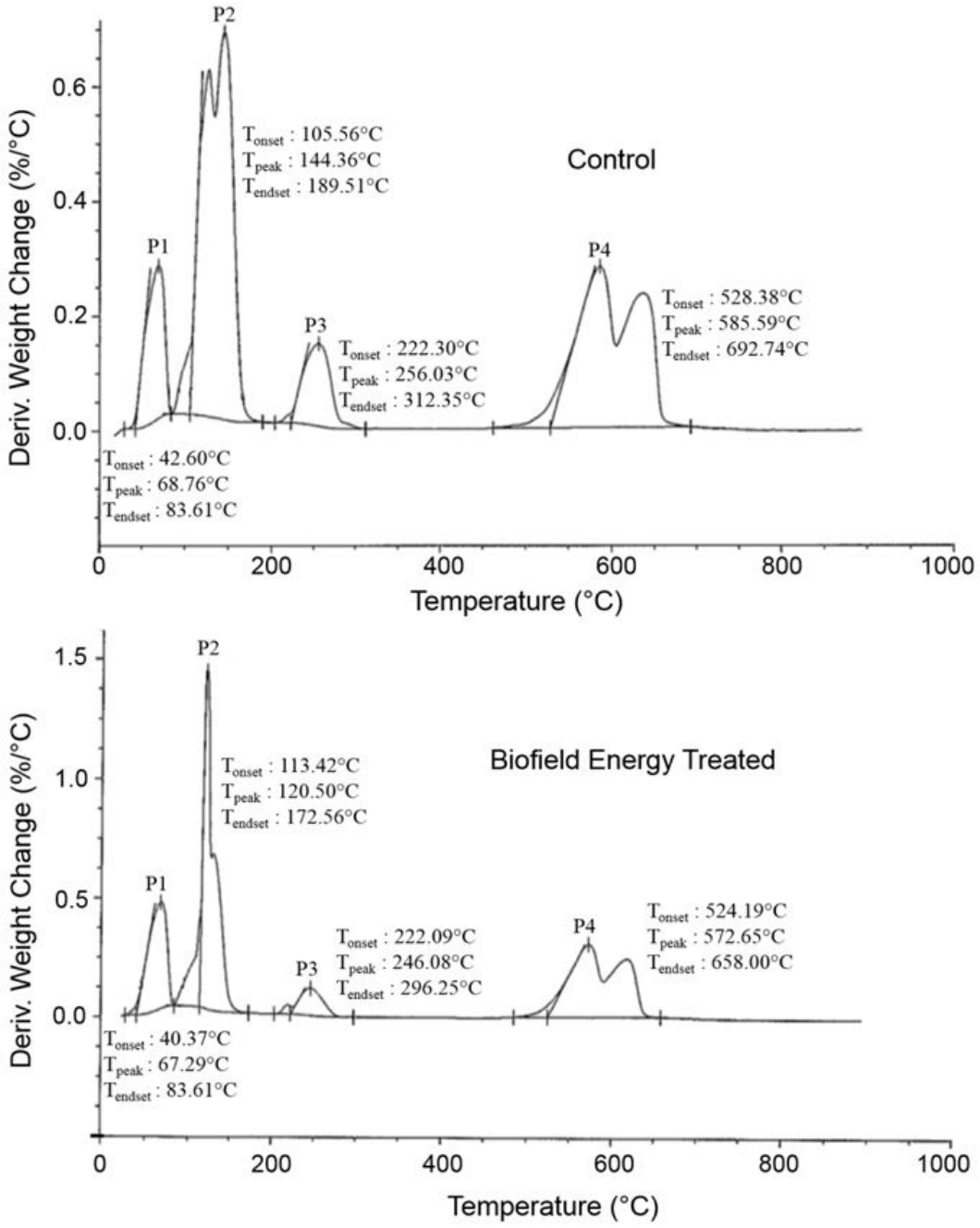

Figure 4: DTG Thermograms of the Control and Treated Sample

Conclusion

The Trivedi Effect® - Consciousness Energy Healing Treatment has the astounding capability to modify the solid state charateristics of ferrous sulphate. The XRD relative peak intensities of the treated sample were significantly changed from -66.93% to 331.88% compared to the control sample. Subsequently, the crystallites size of the Biofield Energy Treated ferrous sulphate were significantly altered from -24.92% to 139.87% compared with the control sample. The particle size in the Biofield Energy Treated ferrous sulphate at d_{10}, d_{50}, d_{90}, and D (4,3) values were significantly reduced by 17.56%, 26.94%, 31.66%, and 28.98%, respectively compared with the control sample. The specific surface area of the Biofield Energy Treated sample was significantly increased by 29.57% compared with the control ferrous sulphate. The melting temperature of the treated sample in the 1st and 3rd peaks was lowered by 4.06% and 2.55% respectively, while enhanced by 8.40% and 0.17% in the 2nd and 4th peaks, respectively compared with the control sample. The latent heat of fusion was significantly reduced by 23.22% in the Biofield Energy Treated sample compared with the control sample. The total weight loss in the Biofield Energy Treated sample was increased by 2.00% compared with the control sample. The T_{max} of the treated ferrous sulphate was decreased by 2.14%, 16.53%, 3.89%, and 2.21% in the 1st, 2nd, 3rd, and 4th peak respectively, compared to the control sample. The Trivedi Effect®-Consciousness Energy Healing Treatment might lead to the production of a polymorphic form of ferrous sulphate having decreased particle size and improved surface area, which might increase the dissolution rate and bioavailability of ferrous sulphate compared with the control sample. The Biofield Energy Treated ferrous sulphate would be suitable to design more efficacious nutraceutical/pharmaceutical formulations, which might offer better therapeutic response against iron deficiency anaemia.

Acknowledgement

The authors are grateful to GVK Biosciences Pvt. Ltd., Trivedi Science, Trivedi Global, Inc., Trivedi Testimonials, and Trivedi Master Wellness for their assistance and support during this work.

References

1. Evans AM (1992) Ore Geology and Industrial Minerals: An Introduction (3rd Edn). Wiley-Blackwell 400.

2. Reddy SN, Rao PS, Ravikumar RV, Reddy BJ, Reddy YP (2001) Spectral investigations on melanterite mineral from France. Spectrochim Acta A Mol Biomol Spectrosc 57: 1283-7.

3. Bandi M, Mallineni SK, Nuvvula S (2017) Clinical applications of ferric sulfate in dentistry: A narrative review. J Conserv Dent 20: 278-81.

4. Leary A, Barthe L, Clavel T, Sanchez C, Oulmi-Castel M, et al. (2016) Pharmacokinetics of ferrous sulphate (Tardyferon®) after single oral dose administration in women with iron deficiency anaemia. Drug Res (Stuttg) 66: 51-6.

5. Jančovičová V, Čeppan M, Havlínová B, M Reháková, Z Jakubíková (2007) Interactions in iron gall inks. Chemical Papers 61: 391-7.

6. Koenig R, Kuhns M (2010) Control of iron chlorosis in ornamental and crop plants. Utah State University, Salt Lake City.

7. Hayyan M, Hashim MA, AlNashef IM (2016) Superoxide ion: generation and chemical implications. Chem Rev 116: 3029-85.

8. Fenton HJH (1894) Oxidation of tartaric acid in presence of iron. J Chem Soc 65: 899-911.

9. Bothara KG (2007) Inorganic Pharmaceutical Chemistry (9th Edn), Nirali Prakashan, Pune, India.

10. Zariwala MG, Somavarapu S, Farnaud S, Renshaw D (2013) Comparison study of oral iron preparations using a human intestinal model. Sci Pharm 81: 1123-39.

11. Zimmermann MB, Hurrell RF (2007) Nutritional iron deficiency. Lancet 370: 511-20.

12. Trivedi MK, Branton A, Trivedi D, Nayak G, Balmer AJ, et al. (2017) Evaluation of physicochemical, thermal, structural, and behavioral properties of magnesium gluconate treated with energy of consciousness (the Trivedi Effect®). J Drug Design Med Chem 3: 5-17.

13. Trivedi MK, Branton A, Trivedi D, Nayak G, Balmer AJ, et al. (2017) Study of the energy of consciousness healing treatment on physical, structural, thermal, and behavioral properties of zinc chloride. Mod Chem 5: 19-28.

14. Trivedi MK, Branton A, Trivedi D, Nayak G, Balmer AJ, et al. (2017) Evaluation of physicochemical, spectral, thermal and behavioral properties of the biofield energy healing treated sodium selenate. Sci J Chem 5: 12-22.

15. Rubik B (2002) The biofield hypothesis: Its biophysical basis and role in medicine. J Altern Complement Med 8: 703-17.

16. Trivedi MK, Branton A, Trivedi D, Nayak G, Plikerd WD, et al. (2017) A systematic study of the biofield energy healing treatment on physicochemical, thermal, structural, and behavioral properties of magnesium gluconate. Int J Bioorg Chem 2: 135-45.

17. Trivedi MK, Tallapragada RM, Branton A, Trivedi D, Nayak G, et al. (2015) Characterization of physical and structural properties of aluminium carbide powder: Impact of biofield treatment. J Aeronaut Aerospace Eng 4: 142.

18. Trivedi MK, Tallapragada RM, Branton A, Trivedi D, Nayak G, et al. (2015) The Potential impact of biofield energy treatment on the atomic and physical properties of antimony tin oxide nanopowder. Am J Optics Photonics 3: 123-8.

19. Trivedi MK, Branton A, Trivedi D, Nayak G, Bairwa K, et al. (2015) Spectroscopic characterization of disulfiram and nicotinic acid after biofield treatment. J Anal Bioanal Tech 6: 265.

20. Trivedi MK, Patil S, Shettigar H, Singh R, Jana S (2015) An impact of biofield treatment on spectroscopic characterization of pharmaceutical compounds. Mod Chem Appl 3: 159.

21. Trivedi MK, Tallapragada RM, Branton A, Trivedi D, Nayak G, et al. (2015) Potential impact of biofield treatment on atomic and physical characteristics of magnesium. Vitam Miner 3: 129.

22. Trivedi MK, Branton A, Trivedi D, Nayak G, Bairwa K, et al. (2015) Impact of biofield treatment on spectroscopic and physicochemical properties of p-nitroaniline. Insights Anal Electrochem 1: 1-8.

23. Trivedi MK, Branton A, Trivedi D, Nayak G, Bairwa K, et al. (2015) Physical, thermal and spectroscopical characterization of biofield treated triphenylmethane: An impact of biofield treatment. J Chromatogr Sep Tech 6: 292.

24. Trivedi MK, Patil S, Shettigar H, Mondal SC, Jana S (2015) Evaluation of biofield modality on viral load of Hepatitis B and C viruses. J Antivir Antiretrovir 7: 083-8.

25. Trivedi MK, Branton A, Trivedi D, Nayak G, Mondal SC, et al. (2015) Impact of biofield energy treatment on soil fertility. Earth Sci 4: 275-9.

26. Trivedi MK, Branton A, Trivedi D, Nayak G, Gangwar M, et al. (2015) Evaluation of vegetative growth parameters in biofield treated bottle gourd (Lagenaria siceraria) and okra (Abelmoschus esculentus), Int J Nutr Food Sci 4: 688-94.

27. Trivedi MK, Patil S, Shettigar H, Gangwar M, Jana S (2015) Antimicrobial Sensitivity Pattern of Pseudomonas fluorescens after Biofield Treatment. J Infect Dis Ther 3: 222.

28. Trivedi MK, Branton A, Trivedi D, Nayak G, Lee AC, et al. (2017) Investigation of physicochemical, spectral, and thermal properties of sodium selenate treated with the Energy of Consciousness (the Trivedi Effect®). Am J Life Sci 5: 27-37.

29. Trivedi MK, Branton A, Trivedi D, Nayak G, Bairwa K, et al. (2015) Physicochemical and spectroscopic properties of biofield energy treated protose. Am J Biomed Life Sci 3: 104-10.

30. Trivedi MK, Branton A, Trivedi D, Nayak G, Bairwa K, et al. (2015) Characterization of physicochemical and spectroscopic properties of biofield energy treated bio peptone. Adv Biosci Bioeng 3: 59-66.

31. Trivedi MK, Branton A, Trivedi D, Nayak G, Mondal SC, et al. (2015) Biochemical differentiation and molecular characterization of biofield treated vibrio parahaemolyticus. Am J Clin Exp Med 3: 260-7.

32. Trivedi MK, Patil S, Shettigar H, Bairwa K, Jana S (2015) Evaluation of phenotyping and genotyping characterization of Serratia marcescens after Biofield Treatment. J Mol Genet Med 9: 179.

33. Trivedi MK, Patil S, Shettigar H, Gangwar M, Jana S (2015) In Vitro evaluation of biofield treatment on cancer biomarkers involved in endometrial and prostate cancer cell lines. J Cancer Sci Ther 7: 253-7.

34. Gupta KR, Askarkar SS, Joshi RR, Padole YF (2015) Solid state properties: Preparation and characterization. Der Pharmacia Sinica 6: 45-64.

35. Storey RA, Ymen I (2011) Solid state characterization of Pharmaceuticals, Wiley-Blackwell, UK.

36. Trivedi MK, Mohan TRR (2016) Biofield energy signals, energy transmission and neutrinos. Am J Mod Phy 5: 172-6.

37. Langford JI, Wilson AJC (1978) Scherrer after sixty years: A survey and some new results in the determination of crystallite size. J Appl Cryst 11: 102-13.

38. Brittain HG (2009) Polymorphism in pharmaceutical solids in Drugs and Pharmaceutical Sciences (2nd Edn), Informa Healthcare USA, Inc., New York.

39. Censi R, Martino PD (2015) Polymorph Impact on the Bioavailability and Stability of Poorly Soluble Drugs. Molecules 20: 18759-76.

40. Zhao Z, Xie M, Li Y, Chen A, Li G, et al. (2015) Formation of curcumin nanoparticles via solution-enhanced dispersion by supercritical CO2. Int J Nanomed 10: 3171-81.

41. Haque PF, Zavabeti A, Zhang B, Datta R, Yin Y, et al. (2019) Ordered intracrystalline pores in planar molybdenum oxide for enhanced alkaline hydrogen evolution. J Mater Chem A 7: 257-68.

42. Khadka P, Ro J, Kim H, Kim I, Kim JT, et al. (2014) Pharmaceutical particle technologies: An approach to improve drug solubility, dissolution and bioavailability. Asian J Pharm Sci 9: 304-16.

43. Wang T, Debelak KA, Roth JA (2007) Dehydration of iron (II) sulfate heptahydrate. Thermochimica Acta 462: 89-93.

44. Földvári M (2011) Handbook of thermogravimetric system of minerals and its use in geological practice, Occasional Papers of the Geological Institute of Hungary, Budapest 213.

45. Zhang M, Efremov MY, Schiettekatte F, Olson EA, Kwan AT, et al. (2000) Size-dependent melting point depression of nanostructures: Nanocalorimetric measurements. Phys Rev B 62: 10548.